Use of Transient EPR Spectroscopy of Excited Triplet State for the Structural Assignment of Bisadducts of Fullerene C_{60}

Luigi Pasimeni,*,† Andreas Hirsch,‡ Iris Lamparth,‡ Andrea Herzog,‡ Michele Maggini,§ Maurizio Prato,|| Carlo Corvaja,† and Gianfranco Scorrano§

Contribution from Centro di Studio sugli Stati Molecolari Radicalici ed Eccitati del CNR, Dipartimento di Chimica Fisica, Università di Padova, Via Loredan, 2, 35131 Padova, Italy, Institut für Organische Chemie Universität Erlangen-Nürnberg, Henkestrasse 42, 91054 Erlangen, Germany, Centro Meccanismi di Reazioni Organiche del CNR, Dipartimento di Chimica Organica, Università di Padova, Via Marzolo, 1, 35131 Padova, Italy, and Dipartimento di Scienze Farmaceutiche, Università di Trieste, Piazzale Europa 1, 34127 Trieste, Italy

Received March 26, 1997. Revised Manuscript Received October 13, 1997[⊗]

Abstract: Transient EPR spectroscopy has been applied to measure the spectra of excited triplet states in two series of fullerene bisadducts. Eight different bisadducts of C_{60} with bis(ethoxycarbonyl)methylene and five bis-*N*-methylpyrrolidines have been analyzed. The D and E parameters of electron dipolar interaction and the populations of the zero field triplet sublevels, accounting for spin polarization, have been determined by spectrum simulation. They appear peculiar for each bisadduct. It is shown that triplet EPR technique represents a useful spectroscopic tool that allows structural assignments to bisadducts of C_{60}.

Introduction

The organic chemistry of fullerenes has evolved into a very lively and fascinating field.[1−4] More and more sophisticated molecular architectures are being assembled with potential applications in different fields.[5] The wealth of information available so far deals mainly with monoaddition products, compounds with well-defined structures which can be isolated and characterized. There is, however, a high potential related to the fact that fullerenes are multifunctional reactants; by controlled additions, several functional groups can be inserted.[6] Regretfully, or maybe for this reason fascinatingly, the multiple functionalization of the fullerenes is a very complicated matter. For example, C_{60}, the most abundant representative of the fullerene family, has 30 double bonds which exhibit the same reactivity. Attack to any of the 30 double bonds produces a single monoaddition product. The first addition reduces the symmetry of the fullerene. For symmetrical addends a second addition can produce up to eight isomeric bisadducts. The isomer distribution is not random, but obeys frontier orbital rules.[7] The isolation of the pure isomers from the bisadduct mixture is a strenuous work, which consists of patient HPLC separations, often using more than one stationary phase.

Once this has been done, another nontrivial problem arises, the attribution of the correct structure of all bisadducts. Crystals suitable for X-ray structure determination are usually difficult to obtain,[8] and structural assignment relies mainly on spectroscopic means. Hawkins et al. used INADEQUATE ^{13}C-NMR spectroscopy on osmium bisadducts of ^{13}C-enriched C_{60}.[9] Hirsch and co-workers established an empirical rule based on a combination of polarity criteria and spectroscopic data. As a matter of fact, the structure of some bisadducts (trans-1 with D_{2h} symmetry and eq with C_s symmetry, see Figure 1) can be unambigously assigned by ^{1}H and ^{13}C NMR due to symmetry considerations.[6a,10]

To assign the structure to isomeric bis-*N*-methylpyrrolidine adducts, Wilson and Schuster proposed a comparison between the UV−vis spectra of their products with those reported by Hirsch.[11] The comparison appears relatively safe for some isomers, but may not be sufficient for others: some of the compounds have very different visible spectra. The same group

* Address correspondence to: L. Pasimeni, Dipartimento di Chimica Fisica, Università di Padova, Via Loredan 2, 35131 Padova, Italy; Fax +39-49-8275135; e-mail Pasimeni@pdchfi.chfi.unipd.it.

† Centro di Studio sugli Stati Molecolari Radicalici ed Eccitati del CNR, Dipartimento di Chimica Fisica, Universtà di Padova.

‡ Institut für Organische Chemie Universität Erlangen-Nürnberg.

§ Centro Meccanismi di Reazioni Organiche, Dipartimento di Chimica Organica, Università di Padova.

|| Dipartimento di Scienze Farmaceutiche, Università di Trieste.

⊗ Abstract published in *Advance ACS Abstracts*, December 1, 1997.

(1) Hirsch, A. *The Chemistry of the Fullerenes*; Thieme: Stuttgart, 1994.

(2) Tetrahedron Symposia-in-Print Number 60. *Fullerene Chem.* (Smith, A. B., Guest Ed.) **1996**, *52*, 14.

(3) *The Chemistry of Fullerenes*; Taylor, R., Ed.; Word Scientific: Singapore, 1995.

(4) Diederich, F.; Thilgen, C. *Science* **1996**, *271*, 317−23.

(5) See, for example: (a) Isaacs, L.; Seiler, P.; Diederich, F. *Angew. Chem., Int. Ed. Engl.* **1995**, *34*, 1466−9. (b) Camps, X.; Schoenberger, H.; Hirsch, A. *Chem. Eur. J.* **1997**, *3*, 561−7.

(6) (a) Hirsch, A.; Lamparth, I.; Karfunkel, H. R. *Angew. Chem., Int. Ed. Engl.* **1994**, *33*, 437−8. (b) Hirsch, A. *J. Chem. Soc., Chem. Commun.* **1994**, 1727−8. (c) Lamparth, I.; Maichle-Mössmer, C.; Hirsch, A. *Angew. Chem., Int. Ed. Engl.* **1995**, *34*, 1607−9. (d) Schick, G.; Hirsch, A.; Mauser, H.; Clark, T. *Chem. Eur. J.* **1996**, *2*, 935−43. (e) Grösser, T.; Prato, M.; Lucchini, V.; Hirsch, A.; Wudl, F. *Angew. Chem., Int. Ed. Engl.* **1995**, *34*, 1343−5. (f) Isaacs, L.; Haldimann, R. F.; Diederich, F. *Angew. Chem., Int. Ed. Engl.* **1994**, *33*, 2339−42. (g) Cardullo, F.; Isaacs, L.; Diederich, F.; Gisselbrecht, J.-P.; Boudon, C.; Gross, M. *Chem. Commun.* **1996**, 797−9. (h) Wilson, S. R.; Lu, Q. *Tetrahedron Lett.* **1995**, *36*, 5707−10.

(7) Hirsch, A.; Lamparth, I.; Schick, G. *Liebigs Ann.* **1996**, 1725−34.

(8) (a) Balch, A. L.; Costa, D. A.; Noll, B. C.; Olmstead, M. M. *J. Am. Chem. Soc.* **1995**, *117*, 8926−32. (b) Balch, A. L.; Ginwalla, A. S.; Olmstead, M. M.; Herbst-Irmer, R. *Tetrahedron* **1996**, *52*, 5021−32. (c) Seiler, O.; Isaacs, L.; Diederich, F. *Helv. Chim. Acta* **1996**, *79*, 1047−58. (d) Kräutler, B.; Müller, T.; Maynollo, J.; Gruber, K.; Kratky, C.; Ochsenbein, P.; Schwartzenbach, D.; Bürgi, H.-B. *Angew. Chem., Int. Ed. Engl.* **1996**, *35*, 1204−6. (e) Kusukawa, T.; Ando, W. *Angew. Chem., Int. Ed. Engl.* **1996**, *35*, 1315−7.

(9) Hawkins, J. M.; Meyer, A.; Lewis, T. A.; Bunz, U.; Nunlist, R.; Ball, G. E.; Ebbesen, T. W.; Tanigaki, K. J. *J. Am. Chem. Soc.* **1992**, *114*, 7954−5.

(10) Djojo, F.; Herzog, A.; Lamparth, I.; Hampel, F.; Hirsch, A. *Chem. Eur. J.* **1996**, 1537−47.

(11) Lu, Q.; Schuster, D. I.; Wilson, S. R. *J. Org. Chem.* **1996**, *61*, 4764−8.

S0002-7863(97)00958-X CCC: $14.00

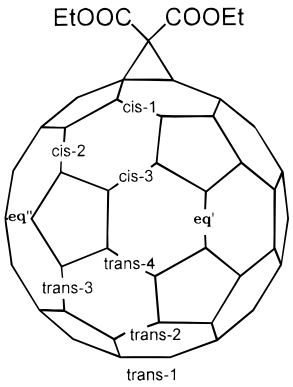

Figure 1. Positional relationships between the 6−6 bonds in C_{60} and the symmetry of the corresponding bisadducts.

has also attempted to correlate the structure of the bisadducts with the ^{3}He chemical shifts in the NMR spectra of ^{3}He@C_{60} fullerene derivatives. However, this approach can still be considered at a rather preliminary stage, and certainly is not of wide applicability.[12] In conclusion, except for rare X-ray determinations,[8] currently there is not an available general method for the attribution of the structure to bisadducts of C_{60}.

In this paper we suggest a new method, based on EPR study of the excited triplet state of the bisadducts. In the ground state, C_{60} possesses 5-fold degenerate HOMO (h_u) and 3-fold degenerate LUMO (t_{1u}) levels.[13] Irradiation with visible light generates excited singlet states which convert into the lowest excited triplet state by means of the spin orbit interaction in a time scale of 10^{-8}−10^{-9} s.[14] In the long-lived triplet state of C_{60} and C_{60} derivatives, the triple spin degeneracy is lifted by electron dipolar interaction, and three separate *X*, *Y*, and *Z* zero field levels result.[15] The intersystem crossing causes selective populations p_x, p_y, and p_z of the zero field energy levels. Their ratio depends on the molecular symmetry in the excited triplet state. When the sample is placed into a magnetic field, as it occurs in EPR spectroscopy, the populations of the triplet Zeeman levels are linear combinations of zero field values, with coefficients depending on the orientation of the magnetic field with respect to the molecular axes. The shape of the EPR spectrum of random-oriented samples of triplet excited molecules depends on the zero field splitting parameters and on the zero field populations. Both represent a useful set of parameters for identifying the structure of fullerene bisadducts.

Two series of C_{60} bisadducts have been considered in this work. Seven adducts are formed and can be isolated from bisaddition of diethyl bromomalonate to C_{60} under basic conditions (Figure 1 and Chart 1, adduct **1**).[6a] Mixed adducts of type **2**, Chart 1,[10] have also been studied for comparison with the **1** series and for the possibility of obtaining a cis-1 isomer, not formed in the case of **1**. Five adducts **3** (Chart 1), have been isolated and characterized from bisaddition of *N*-methylazomethine ylides to C_{60}.

Experimental Section

Instrumentation. ^{1}H and ^{13}C NMR spectra were recorded on a Bruker AC 250 spectrometer. Chemical shifts are given in parts per million (δ) relative to tetramethylsilane. MALDI (matrix-assisted laser desorption ionization) mass spectra were obtained in positive linear mode at 15 KV acceleration voltage on a mass spectrometer Reflex time of flight (Bruker), using 2,5-dihydroxybenzoic acid as matrix. APCI (atmospheric pressure chemical ionization) mass spectra were recorded on a Perkin-Elmer AP1-Sciex spectrometer. Reactions were monitored by thin-layer chromatography using Merck precoated silica gel (0.25 mm thickness) plates. Flash column chromatography was performed employing 230−400 mesh silica gel (Merck). Purification of bisadducts **3a**−**e** was accomplished by HPLC using a Primesphere silica column from Phenomenex (250 × 10 mm, 5 μm). Isocratic elution was performed on a LC pump unit Shimadzu LC-8A at a flow rate of 2 mL min^{-1} with HPLC-grade toluene/ethyl acetate mixtures as the mobile phase. The elution was monitored with a Shimadzu SPD-6A UV spectrophotometric detector at 340 nm.

Toluene solutions of the fullerene adduct (5×10^{-4} M) for EPR measurements were carefully degassed and sealed under vacuum in quartz tubes of 3 mm inner diameter. Photoexcited paramagnetic states were detected by time resolved EPR spectroscopy, i.e. laser excitation and time-resolved direct detection (DD) in continuous wave microwave field. In DD experiments the sample was placed in the microwave TE_{102} rectangular cavity of the EPR spectrometer (Bruker ER 200 D X-band) and irradiated by a Lambda Physik LPX 100 XeCl excimer laser (λ = 308 nm, ∼10 mJ/pulse), which fed a Rhodamin G6 dye laser with emitting light at 581 nm (pulse duration ∼20 ns). The signal was taken directly from the microwave preamplifier immediately after the detection diode and fed into an EG&G Boxcar Averager mod. 162 equipped with a mod. 164 plug-in. While the magnetic field was swept, the averager was activated ∼0.5 μs after the laser pulse, corresponding nearly to the maximum of the transient signal. It was operative with an integration window of 50 ns. Temperature was controlled by an Oxford ESR-900 helium continuous flow cryostat. The spectra were recorded at 20 K.

Materials. C_{60} was purchased from Bucky USA (99.5%). All other reagents were used as purchased from Fluka and Aldrich. All solvents were distilled prior to use.

The synthesis of the bisadducts **1**[6a] and **2**[10] have been already reported.

Synthesis of Bis-*N*-methylpyrrolidine Derivatives 3a−e. A solution of 146 mg of *N*-methylpyrrolidine monoadduct (0.18 mmol), 66 mg (0.74 mmol) of *N*-methylglycine, and 24 mg (0.80 mmol) of paraformaldehyde in 150 mL of toluene was heated to reflux for 4 h. The solution was concentrated under reduced pressure, and *N*-methylpyrrolidine bisadducts were purified from unreacted *N*-methylpyrrolidine monoadduct (30 mg, 20%) and higher adducts by flash column chromatography on silica gel using toluene as eluent. A fraction containing bisadducts **3a**−**c** (mixture 1) was eluted with toluene/ethyl acetate, 95:5, and then a fraction with the other bisadducts **3d** and **3e**, as major components (mixture 2), was collected employing toluene/ethyl acetate, 7:3. Complete separation of bisadducts in mixtures 1 and 2 was accomplished on a semipreparative HPLC silica column using toluene/ethyl acetate, 9:1, to elute **3a**−**c** (yield: **3a**, 1.5%; **3b**, 6.5%; **3c**, 5.5%) and toluene/ethyl acetate, 1:1, to elute **3d**−**e** (yield: **3d**, 6.8%; **3e**, 6.5%). **3e**: ^{1}H NMR (250 MHz, $CDCl_3$) δ (ppm) 2.63 (s, 3H), 2.64 (s, 3H), 3.73 (s, 2H), 3.88 (s, 2H), 3.77, 3.81, 3.88, 3.91 (AB quartet, 4H); ^{13}C NMR (62.9 MHz, CD_2Cl_2) δ (ppm) 41.29 (1C), 41.43 (1C), 69.07 (1C), 69.69 (1C), 70.00 (2C), 70.05 (1C), 70.19 (1C), 70.42 (2C), 135.79 (2C), 136.89 (2C), 139.37 (2C), 140.86 (2C), 141.58 (2C), 141.74 (2C), 141.98 (2C), 143.30 (2C), 143.84 (2C), 144.51 (2C), 144.75 (2C), 144.76 (2C), 145.12 (2C), 145.34 (2C), 145.85 (2C), 146.71 (2C), 146.83 (2C), 147.29 (4C), 147.83 (2C), 148.18 (2C), 148.96 (2C), 149.84 (1C), 152.81 (2C), 153.06 (2C), 153.62 (2C), 155.20 (2C), 155.99 (1C), 159.04 (2C); UV−vis (cyclohexane) λ_{max} 226, 243, 264, 412, 447, 640, 705; MALDI-MS $C_{66}H_{14}N_2$ (MW = 834) *m*/*z* 834 $[M]^+$.

During the purification of mixture 2, small amounts of three other adducts, possessing elution times shorter than **3e**, were also separated and found to be trisadducts from MALDI-MS [$C_{69}H_{21}N_3$ (MW = 891) *m*/*z* 891 $[M]^+$] and API-MS [toluene/MeOH/HCO_2H, *m*/*z* 892 $[M + H]^+$].

(12) Cross, J.; Jimenez-Vazquez, H. A.; Lu, Q.; Saunders, M.; Schuster, D. I.; Wilson, S. R.; Zhao, H. *J. Am. Chem. Soc.* **1996**, 11454−9.

(13) Haddon, R. C. *Acc. Chem. Res.* **1992**, *25*, 127−33.

(14) (a) Arbogast, J. W.; Darmanian, A. P.; Foote, C. S.; Rubin, Y.; Diederich, F. N.; Alvarez, M. M.; Anz, S. J.; Whetten, R. L. *J. Phys. Chem.* **1991**, *95*, 11−2. (b) Williams, R. M.; Zwier, J. M.; Verhoeven J. W. *J. Am. Chem. Soc.* **1995**, *117*, 4093−9.

(15) Wasielewski, M. R.; O'Neill, M. P.; Lykke, K. R.; Pellin, M. J.; Gruen, D. M. *J. Am. Chem. Soc.* **1991**, *113*, 2774−6.

Chart 1

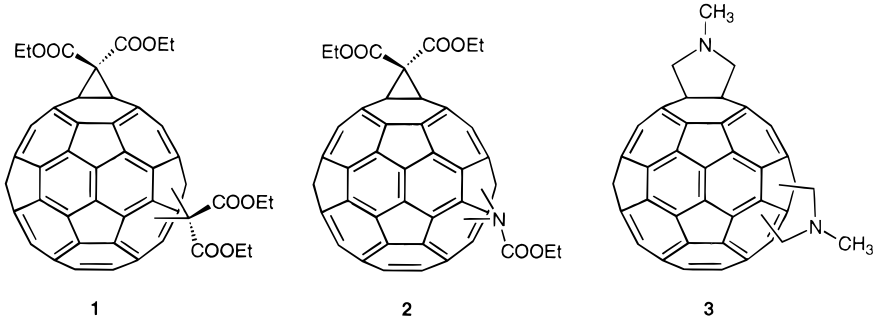

Results

A first series of experiments were performed on **1** and **2**. The cyclopropanation of C_{60} with diethyl bromomalonate gives rise to seven isomers of $C_{62}(COOEt)_4$ which have been already characterized by UV−vis and NMR spectroscopies.[6a,10] The **1h** isomer was not formed in contrast to **2h** ($C_{61}(COOEt)_2$-NCOOEt), which is a preferred adduct due to the lack of sterical hindrance. The spatial arrangement of the added groups for both types of adducts is sketched in Figure 1.

We have also recorded the EPR spectra of the two equatorial **2e** isomers denoted as eq′ and eq″ of the bisadduct having the $C(COOEt)_2$ residue replaced by N(COOEt), shown in Figure 1.

A second set of experiments were performed on a series of regioisomeric bis-*N*-methylpyrrolidines **3** prepared starting from *N*-methylpyrrolidine monoadduct, sarcosine, and paraformaldehyde in refluxing toluene and purified using a combination of flash chromatography and semipreparative HPLC (silica gel, toluene/ethyl acetate mixtures). Five bisadducts **3a**−**e** were isolated and tentatively assigned to trans-1, trans-2, trans-3, trans-4, and eq, respectively, on the basis of their retention factor $k' = (t - t_0)/t_0$, calculated from HPLC data. The k' value increases from **3a** through **3e** as one expects considering that the electric dipole of the molecule increases going from trans-1 through eq.

MALDI and API mass spectrometry confirmed that **3a**−**e** are *N*-methylpyrrolidine bisadducts. On the basis of symmetry considerations, ^{1}H and ^{13}C NMR analyses allow unequivocal structure determination of trans-1, the only D_{2h}-symmetrical isomer, and eq that belongs to the C_s symmetry group.

Two singlets at 2.94 (CH_3) and 4.48 ppm (CH_2) were found in the proton spectrum of **3a**, consistent with the high symmetry of isomer trans-1. These data, along with UV−vis spectral features in the 400−700 nm region, match those found by Lu et al.[11]

The peculiar NMR features of isomer **3e** reflect those expected for an equatorial bisadduct. The ^{1}H NMR spectrum of **3e** shows in fact two singlets at 2.63 and 2.64 ppm (CH_3 groups), two singlets at 3.73 and 3.88 ppm (two CH_2 groups), and a AB quartet for the remaining two CH_2 groups (see the Experimental Section). The ^{13}C NMR spectrum shows 28 signals (25 integrate two carbons, one integrates four carbons, and two integrate one carbon) between 135 and 160 ppm as well as two peaks at 41.29 and 41.43 ppm (CH_3), two peaks at 69.07 and 69.69 ppm (one carbon each, CH_2), one peak at 70 ppm (two carbons, CH_2), and three peaks at 70.05, 70.19, and 70.42 ppm relative to sp^3 fullerene carbons (the latter integrates two carbons). These findings are consistent with an equatorial structure for **3e**. It is worth noting that this adduct was not seen by Lu et al.[11]

The ^{13}C NMR spectrum of each regioisomer **3b** and **3c** shows 28 sp^2 fullerene carbons between 134 and 160 ppm, consistent with the C_2 symmetry of trans-2 and trans-3 whereas that of **3d** displays up to 30 sp^2 fullerene carbons between 128 and 156 ppm compatible with the C_s symmetry of trans-4. These results corroborate the structural assignment to these compounds reported by Lu et al.[11]

Three other compounds, possessing elution times shorter than **3e**, were also separated and found to be triadducts from MALDI and API-MS. This means that, under our chromatographic conditions, *N*-methylpyrrolidine trisadducts are eluted together with bisadducts. To the best of our knowledge, this is the first case of such an event (trisadducts coeluting with bisadducts), which adds more difficulties to the isomers' isolation and relative structural assignment. For this reason, we cannot rule out the formation of cis bisadducts in the reaction mixture. They should be still more polar than **3e**, and therefore might be hidden somewhere under higher adducts.

All samples gave highly polarized transient EPR spectra, which are represented in Figures 2−5 together with their computer simulations.

The spin Hamiltonian for a triplet state molecule is

$$H = g\beta \mathbf{S}\cdot\mathbf{B} - (XS_x^2 + YS_y^2 + ZS_z^2)$$

where X, Y, and Z are the eigenvalues of the fine structure tensor and *x*, *y*, *z* are the eigenvectors. Here, we denote by *X* the smallest component in absolute value.

Because the fine structure tensor is traceless, the spin Hamiltonian can be written in terms of only two parameters, $D = -^3/_2 Z$ and $E = {}^1/_2(Y - X)$, called zero field splitting (zfs) parameters, which characterize the strength and the asymmetry of the electron dipolar coupling. The total width of the powder EPR spectrum is 2*D*, and the shape depends on the values of *D* and *E* and on the spin polarization carried by the transitions.

The polarization of each transition can be calculated for every molecular orientation in the magnetic field from the population of the zero field energy levels p_x, p_y, and p_z of the triplet levels at zero field. The line shape of the powder spectrum is then obtained integrating for the weighted contribution of the molecules which depends on the orientation of the molecular axes with respect to the external magnetic field **B**.[16] Calculations were performed for different sets of *D*, *E*, and population parameters.

The best fit to the experimental spectra of series **1** and of **2h** is represented in Figure 2 by dashed lines. Change of ±1 G in the *D*, *E* values gives a significant worsening in the matching of experimental and calculated spectra.

The obtained fine structure values *D* and *E* and zero field populations are listed in Table 1.

We note that the triplet EPR technique can be useful in displaying the degree of purity of the isomers. In fact, in an

(16) Gonen, O.; Levanon, H. *J. Phys. Chem.* **1984**, *88*, 4223−8.

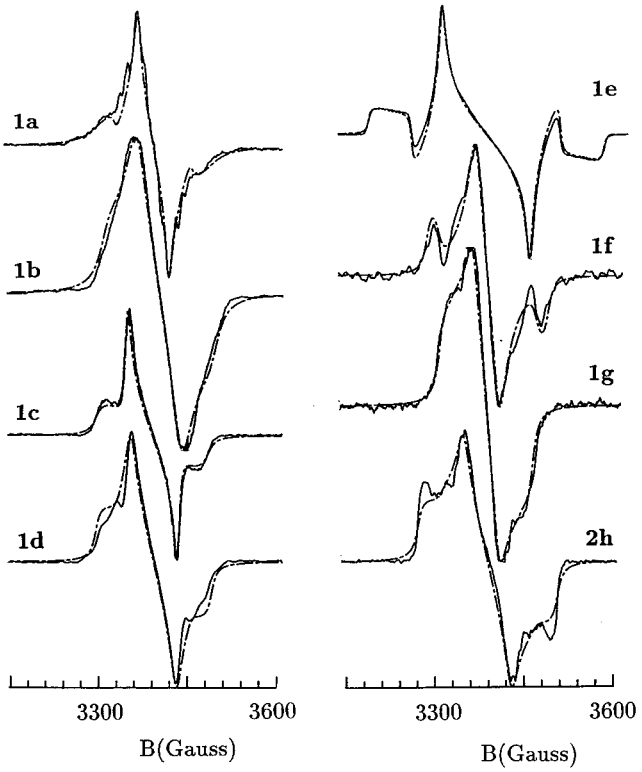

Figure 2. Experimental (solid line) and simulated (dash-dotted line) EPR spectra of bisadduct **2h** of series **2** and of the other seven bisadducts of series **1** as indicated in Figure 1.

Table 1. *D* and *E* Parameters (in Gauss) and Population Ratios of the Lowest Excited Triplet State in Bisadducts of Series **1** and **2**[a]

bisadduct	*D*	*E*	$(p_x - p_y):(p_y - p_z)$	structure
monoadduct	−99	−2	1:0.33	
1a	−91	−13	1:0.48	trans-1
1b	−88	−4	1:0.64	trans-2
1c	−94	−2	1:0.12	trans-3
1d	−96	−5	1:0.07	trans-4
1e	−199	−17	1:0.10	eq
2e′	−195	−12	1:0.10	eq′
2e″	−196	−15	1:0.10	eq″
1f	−102	−21	1:0.07	cis-3
1g	−78	−13	1:0.54	cis-2
2h	−117	−13	1:0.54	cis-1

[a] for equatorial bisadducts *eq′* and *eq″*, see Figure 1. Estimated error limit in the *D* and *E* values is ±1 G.

attempt to study isomer **1a**, which contains **1e** as an impurity, we detected the spectrum represented in Figure 3, which was reproduced as due to the superpositon of spectra belonging to the pure **1a** and **1e** isomers.

Another interesting observation was made for **1c** and **2c** isomers. When the toluene solution is slowly cooled in the spectrometer cavity, the spectrum contains additional lines corresponding to triplet spectra with smaller $|D|$ values. Upon fast cooling, the inner lines disappear. The low field part of the **2c** spectrum is represented in Figure 4, which contains also the lines from the additional spectra. We assign these spectra to triplet excitations over molecule aggregates grown during the slow cooling.[17,18]

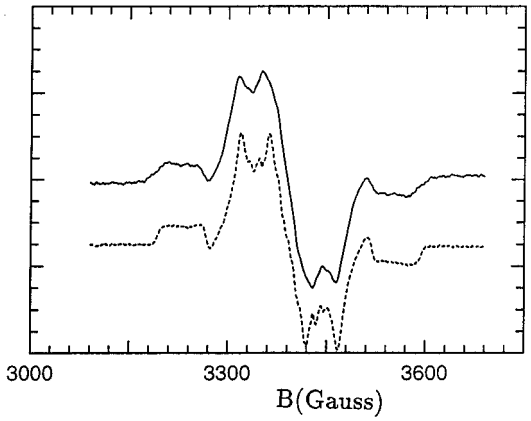

Figure 3. (a) EPR spectrum of crude trans-1 material and (b) the sum (1:1) spectrum of pure trans-1 and eq bisadducts of series **1**.

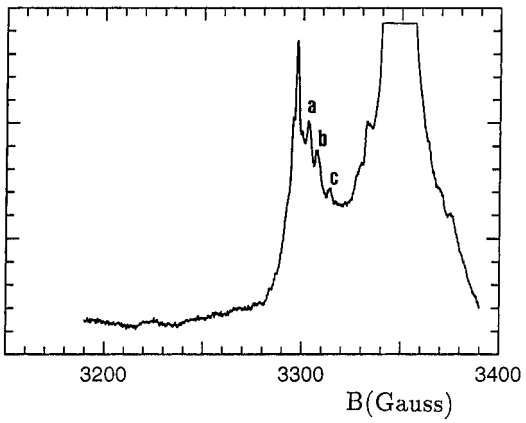

Figure 4. The low field part of the EPR spectrum for bisadduct **2c**. Peaks a, b, and c indicate the low-field outermost line of the additional triplet spectra. The corresponding *D* values are 87 (a), 84 (b), and 78 (c).

We have also observed that samples of **3c** subjected to rapid cooling in the spectrometer cavity give rise to spectra that contain additional inner lines attributed to aggregated species. Two other additional spectra characterized by $|D|$ values 69 and 87 G were identified by spectrum simulation.

Experimental and simulated EPR spectra of **3a**−**e** bisadducts are represented in Figure 5, while the zfs parameters and the population ratios are collected in Table 2 together with those of the C_{60} and *N*-methylpyrrolidine monoadduct.

Discussion

The structure assigned to each bisadduct is reported in Table 2. Bisadducts **3a** and **3e** are unequivocally assigned to the trans-1 and the equatorial structure on the basis of their NMR spectra. The assignment is confirmed by the analysis of triplet EPR spectra whose *D* and *E* values compare well with those of the corresponding bisadducts **1a** and **1e** reported in Table 1. Bisadducts **3b**, **3c**, and **3d** are assigned to trans-2, trans-3, and trans-4 by comparison with the EPR spectra of compounds of the series **1** and on the basis of their retention factor *k′*.

It should be stressed that, apart from slight changes in the zfs parameters due to the different nature of the addends, the data of Table 2 compare well with all those reported in Table 1.

(17) (a) Groenen, E. J. J.; Poluetkov, O. G.; Matsushita, M.; Schmidt, J.; van der Waals, J. H. *Chem. Phys. Lett.* **1992**, *197*, 314−8. (b) van der Heuvel, D. J.; Chan, I. Y.; Groenen, E. J. J.; Schmidt, J.; Meijer, G. *Chem. Phys. Lett.* **1994**, *231*, 111−8. (c) van der Heuvel, D. J.; Chan, I. Y.; Groenen, E. J. J.; Matsushita, M.; Schmidt J.; Meijer, G. *Chem. Phys. Lett.* **1995**, *233*, 284−90.

(18) Bennati, M.; Grupp, A.; Mehring, M. *J. Chem. Phys.* **1995**, *102*, 9457−64.

(19) (a) Maggini, M.; Scorrano, G.; Prato, M. *J. Am. Chem. Soc.* **1993**, *115*, 9798−9.

(20) Agostini, G.; Corvaja, C.; Pasimeni, L. *Chem. Phys.* **1996**, *202*, 349−56.

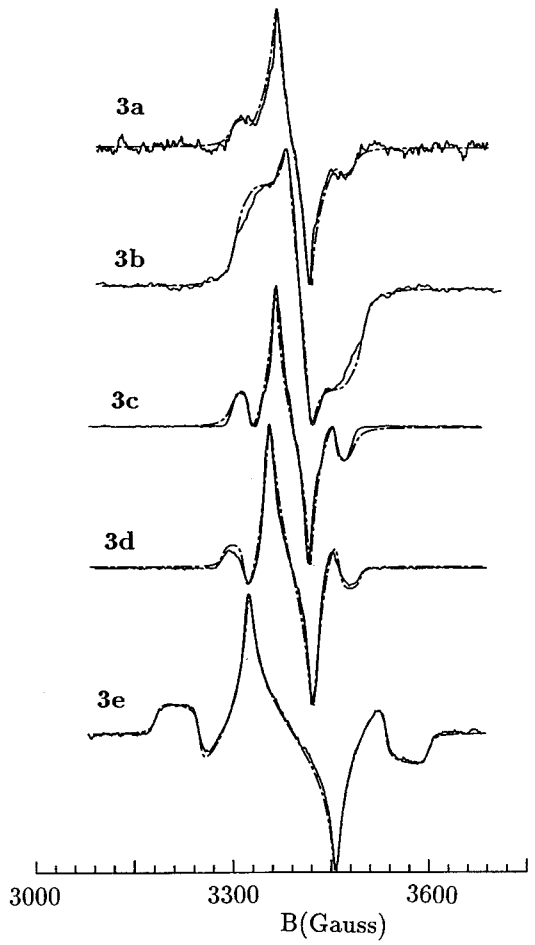

Figure 5. Experimental (solid line) and simulated (dash-dotted line) EPR spectra of the bisadducts of series **3**. Order of elution and NMR and EPR spectra support the indicated structure assignment.

Table 2. *D* and *E* Parameters (in Gauss) and Population Ratios of the Lowest Excited Triplet State in Bisadducts of **3**[a]

bisadduct	*D*	*E*	$(p_x - p_z):(p_y - p_z)$	structure
monoadduct[22,23]	−96	−15	1:0.28	
3a	−95	−15	1:0.38	trans-1
3b	−97	−19	1:0.64	trans-2
3c	−93	−13	1:0.15	trans-3
3d	−105	−13	1:0.05	trans-4
3e	−208	−25	1:0.00	eq

[a] Structure of the adduct supported by order of elution, NMR and EPR spectra is listed. Estimated error limit in the *D* and *E* values is ±1 G.

As shown in Figure 2, all EPR spectra of bisadducts **1** and **2** show the same polarization pattern, i.e. absorptive peaks at the low field side and emissive peaks at the high field side. The polarization pattern coincides with that observed for the monoadduct and for C_{60}. For the latter, EPR spectra can be reproduced by the two sets of parameters: (1) $D > 0$ and p_x, $p_y < p_z$; (2) $D < 0$ and p_x, $p_y > p_z$. The sign of *D* for $^3C_{60}$ has been determined experimentally from ENDOR measurements and proven to be negative.[21] Therefore, a negative sign of *D* combined with p_x, $p_y > p_z$ has been used to simulate the polarized EPR spectrum of $^3C_{60}$.

The list of zfs parameters of **1** and **2** bisadducts reported in Table 1 shows that the *D* and *E* values scatter in a rather narrow range, including those for monoadduct and C_{60}. The equatorial bisadduct, which exhibits a considerably larger *D* value, is an exception. However, on closer inspection, the whole set of parameters for each adduct appears sufficient to be used as fingerprint to identify particular bisadducts. In fact, cis-1 and cis-2 display the same zero field populations but differ markedly in the *D* values. Likewise, cis-3 is discernable from cis-1 and from cis-2 for *D*, *E*, and $p_y - p_z$ values.

Instead, identification of trans bisadducts appears more challenging. Nevertheless, trans-1 is characterized by the largest asymmetry *E* value among the trans series and trans-2 has the largest $p_y - p_z$ value among the trans series. Trans-3 and trans-4 bisadducts give almost coincident spectra, but their identification can rely on other sources of information (C_s vs C_2 symmetry, respectively).

We note that on going from the bisadducts of series **1** to those of series **2**, minor changes in the zfs and population parameters are observed as shown by the data collected in Table 1.

Comparison of data collected in Tables 1 and 2 indicates that the triplet EPR spectra of the trans bisadducts of series **3** present a close similarity in the trend of the $p_y - p_z$ values with respect to the corresponding bisadducts **1a**−**d**. Instead, apart from trans-1, zfs parameters of **3** show some differences in comparison with those of **1** like a steadily smaller *E* value. In the series **1b**−**d** one observes as well a smooth increase of *D* which is not noted in series **3**.

For both series, monoadduct and trans-1 bisadduct have *D* values quite similar to that of $^3C_{60}$. In order to account for such similarities, we observe that the monoadduct has C_{2v} symmetry and trans-1 has D_{2h} symmetry. For both compounds the 2-fold symmetry *z* axis passes through the middle of one or both of the opposite fullerene 6−6 ring junctions at apical positions. The value and sign of *D* depend on the triplet wave function over the surface of the fullerene molecule in the excited state. For $^3C_{60}$ it is expected a spin density maximum near the equatorial plane of the molecule normal to one of the 2-fold axes of the C_{60} icosahedral symmetry. In the monoadduct and trans-1 bisadduct it is assumed that such 2-fold symmetry axis is maintained. The C_2 symmetry axis of the ground state is maintained in the excited triplet state, representing the *z* axis of the dipolar interaction. In the monoadduct and trans-1 bisadduct, the apical positions over C_{60} sphere are involved, such positions lying in the nodal plane of the spin density distribution.

Account of the zfs parameters in the other bisadducts should require a detailed knowledge of triplet wave function. However, some speculations are possible on the basis of symmetry considerations. The eight bisadduct isomers are grouped into three subsets charecterized by D_{2h}, C_2, or C_s symmetry. In the first two cases one principal axis of dipolar interaction coincides with the 2-fold axis.

Recently,[23] we have performed a model calculation of the *D* parameter that makes use of the unpaired electron distribution of the triplet state and is based on a model of fully localized C−C double bonds over the fullerene surface. The zfs parameter *D* is obtained as a sum of the contributions from all the C−C double bonds. For $^3C_{60}$, contribution to the *D* value is given mainly by the bonds straddling the equatorial plane.

The set of *D* values from cis and trans isomers suggest that the *z* axis is arranged in such a way that the corresponding equatorial plane does not bisect bonds engaged by addends. Moreover, for the equatorial bisadduct addends effect a pinning of the triplet wave function in that plane.

(21) Groenen, E. J. J. Private communication.

(22) The population ratios for monoadduct shown in Table 2 differ from those previously reported (1:0.85:0.03) which were obtained from light modulation−field modulation EPR spectra.[23] In the latter case p_x:p_y:p_z represent stationary values and are affected by spin−lattice relaxation and chemical decay.

(23) Agostini, G.; Corvaja, C.; Maggini, M.; Pasimeni, L.; Prato, M. *J. Phys. Chem.* **1996**, *100*, 13416−20.

Conclusion

We have shown that the EPR spectra of excited triplet states in fullerene bisadducts are a valuable tool in the structural assignment. In most cases it is possible to unambigously identify the addition pattern by comparing the zfs and population parameters of different bisadducts.

Compared to UV−visible and NMR spectroscopies, application of the triplet EPR technique appears to be unique in the case of mixtures or impure materials. It should also be useful to allow structural assignment to bisadducts of C_{60} when addends are unsymmetrical or two different groups have been added sequentially.

Acknowledgment. Some of this work was supported by the CNR (Progetto Strategico Materiali Innovativi). We thank Dr. A. Bandiera and Prof. V. Giancotti for their help in API-MS and Dr. R. Seraglia for MALDI-MS data. We are grateful to Dr. S. Zanellato for his help with detailed synthetic procedures.

JA9709583